Hindawi
Advances in Civil Engineering
Volume 2020, Article ID 8829651, 18 pages
https://doi.org/10.1155/2020/8829651

Research Article

Stabilization Mechanism and Safety Control Strategy of the Deep Roadway with Complex Stress

Yang Yu,[1] Dingchao Chen,[1] Xiangqian Zhao,[1] Xiangyu Wang,[2] Lianying Zhang,[1] and Siyu Zhu[1]

[1]*College of Civil Engineering, Xuzhou University of Technology, Xuzhou, Jiangsu 221111, China*
[2]*School of Mines, China University of Mining & Technology, Xuzhou, Jiangsu 221116, China*

Correspondence should be addressed to Dingchao Chen; 20170702129@xzit.edu.cn

Received 22 June 2020; Revised 1 August 2020; Accepted 25 August 2020; Published 4 September 2020

Academic Editor: Bisheng Wu

With the increase of mining intensity of coal resources, some coal mines in China have gradually entered the deep mining stage. The complexity of the stress environment of the deep rock stratum leads to the difficulty of coal mining. Among them, the control of the deep roadway is one of the bottlenecks restricting the safety mining of the deep coal resources in China. By means of statistical analysis, the factors affecting the stability of the deep roadway were summed up: roadway occurrence environment, driving disturbance, and support means. The mechanical model of the deep roadway was established with the theory of elastic-plastic mechanics, the distribution characteristics of the plastic zone of the roadway were revealed, and the influence laws of lateral pressure coefficient, vertical stress, and support strength on the stability of the roadway were analyzed. Through numerical simulation, the law of stress, displacement and the plastic zone distribution evolution of the deep roadway, the mechanism of horizontal stress, and the mechanism of bolt support on the roadway were studied. On this basis, the safety control strategies to ensure the stability of the deep roadway were put forward: improving the strength of the roof and floor, especially the bearing part of the top angle and the side angle, enhancing the stability of the two sides of the roadway and controlling the floor heave, and making the surrounding rock of the deep roadway release pressure moderately, so as to make the roadway easy to be maintained under the low stress environment. These meaningful references were provided for the exploitation of deep coal resources in China.

1. Introduction

When human beings are exploring the space of the celestial body, they are expanding their exploration towards the deep of Earth at the same time, and mining engineering is the largest engineering of human beings under the deep of ground. With the enhancement of the intensity of resource exploration and development, mining is developing towards stratum under kilometers or even deeper stratum. At present, Chinese coal mining is expanding towards deeper ground in an average speed of 8–12 meters per year, and it can be predicted that deep well with kilometers shall be the main source of Chinese coal resources [1–5]. However, deep mining of coal mine presents a series of problems, such as the increase of the rock stress, the complexity of tectonic stress, intense exploiting disturbance, and the deterioration of the stability of rock mass, which results in large deformation and serious destruction of the surrounding rock of the deep roadway, and brings in enormous threat to the safe and effective mining of deep mine. Therefore, the difficulty of controlling the surrounding rock of the deep roadway has been one of the main problems of restricting Chinese coal mining to develop to deeper part [6–10]. In allusion to deep mining and controlling the surrounding rock of the roadway, large amount of research results has been studied by scholars at home and abroad, and a certain number of research achievements have been obtained. Hou [11–13] identified the factors affecting the stability of the surrounding rock of the roadway, analyzed the influence of each influencing factor on the stability of the surrounding rock of the roadway, proposed to improve the stress state of the surrounding rock of the roadway and the mechanical

properties of the surrounding rock, rationally selected the support type of the roadway, and improved resistance and optimization of cross section of the roadway which are effective ways to control the surrounding rock of the deep roadway; Kang et al. [14–17] proposed a theory of high prestress and strong support for deep, complex, and difficult roadways in coal mines, developed a high prestress and strong support system, and successfully applied it to the 1,000 meter deep mine roadway in Xinwen mining area. For the problem that traditional rigid anchors cannot adapt to large deformation roadways, He and Guo [18, 19] have developed a constant-resistance large-deformation anchor that can provide constant working resistance and stable deformation. The anchor is suitable for soft rocks and deep roadways and can effectively control the impact of pressure engineering disasters; Bai and Hou [20–22] studied the stability of surrounding rock in deep roadways and proposed the basic methods of controlling the surrounding rock in deep roadways by increasing the strength of the surrounding rocks, transferring high stresses from the surrounding rocks, and adopting reasonable support technologies; Wang et al. [23, 24] studied the influence of support resistance on the deformation and plastic area of the surrounding rock in deep high-stress roadways and proposed that the supporting structure should meet the principle of coordinated support for large deformation of the surrounding rock. The comprehensive control technology based on "truss anchor cable" and anchor cable reinforcement is better to control the surrounding rock stability of the roadway; Li et al. [25] found that there was a regional rupture phenomenon between the fractured zone and the complete zone in the surrounding rock of the deep roadway, and it was successfully monitored by a drilling television imager in a kilometer deep well in the Huainan mining area. The research results of this phenomenon are of great significance for understanding the fracture mode and stability support of the surrounding rock in deep roadways. In response to the shortcomings of ordinary grouting in deep soft rock roadways, Liu et al. [26–29] proposed the use of a three-step grouting process to strengthen surrounding rocks, discussed the three-step grouting slurry diffusion mechanism, and carried out grouting project with the three-step grouting process; Chang and Xie [30–32] analyzed the stress evolution characteristics and deformation failure rules of the surrounding rock after the excavation of the deep rock lane, revealed the stability control mechanism of the surrounding rock in the deep well rock lane, and proposed grouting reinforcement support technology of the deep roadway with the rigid-flexible coupling of the anchor-net cable; Long [33–36] proposed the coanchoring mechanism of the surrounding rock of the deep roadway in view of the problems encountered in the control of the surrounding rock of the deep roadway and established the synergy mechanism with the structure synergy, strength synergy, stiffness synergy, anchoring timing synergy, pretension force synergy, and deformation synergy; Zuo et al. [37–40] believes that the stress gradient is an important factor that causes the surrounding rock failure of the roadway. Based on this, a theoretical model of the gradient failure of the surrounding rock failure in the deep roadway is established, and the relationship between the relative stress gradient and the average tangential stress level provided by the surrounding rock mass is determined.

However, it is still weak in aspects of the mechanism of horizontal stress, deformation and fracture feature of the roadway, and mechanism of bolt support. Thus, this paper established the mechanical model of the deep roadway through theoretical calculation and revealed the distribution characteristic of the plastic zone of the roadway on the basis of analyzing the influencing factors of stability of the surrounding rock of the deep roadway. It also researched the deformation and fracture of the deep roadway, distribution rule of stress evolution, the mechanism of horizontal stress, and the mechanism of bolt support to the deep roadway by the numerical calculation method, based on which it purposefully proposed the safety control countermeasures of the deep roadway.

2. Engineering Background

Shoushan coal mine is about 25 km from Pingdingshan City in Henan province of China, geographical coordinates: 113°21′16″ to 113°26′22″ east longitude and 33°45′45″ to 33°50′52″ north latitude. The well field is 14.5 km long from east to west and 1.1–4.6 km wide from north to south, with an area of 47 km^2. Shoushan coal mine is exploiting No. 15 coal seam whose average burial depth is 750 m, dip angle is 8–12°, and thickness is 3–4 m, with well-field geologic structure development and belongs to high gas extruding mine. No. 15 coal seam has the tendency of spontaneous combustion and the danger of coal dust explosion. The deformation and fracture of the roadway is serious under the combined action of high ground stress and tectonic stress, especially the deformation of floor heave and roof sink is extremely serious after excavation and mining disturbance. It forms vicious spiral of repairing after excavation in the roadway, which threats the safety production of mine seriously. The deformation and fracture situation of the roadway is shown in Figure 1.

In order to provide reliable basic parameters of rock stratum for subsequent theoretical calculation and numerical modeling, so as to reveal the deformation and stability mechanism of the deep roadway, it needs to measure physical and mechanical properties and relevant parameters by extracting No. 15 coal seam and rock samples of roof and floor. The experimental process is shown in Figure 2, and the test result is given in Table 1.

3. Influence Factors of the Stability of the Deep Roadway

The stability of the roadway under deep mining condition not only relates with the lithology and intensity of the surrounding rock but also is influenced by external stress environment. These influence factors mainly include occurrence environment, excavation disturbance, and support means.

3.1. Occurrence Environment. Ground stress is the basic parameter of the roadway stability and the design of supporting structure. The existence of tectonic stress field or

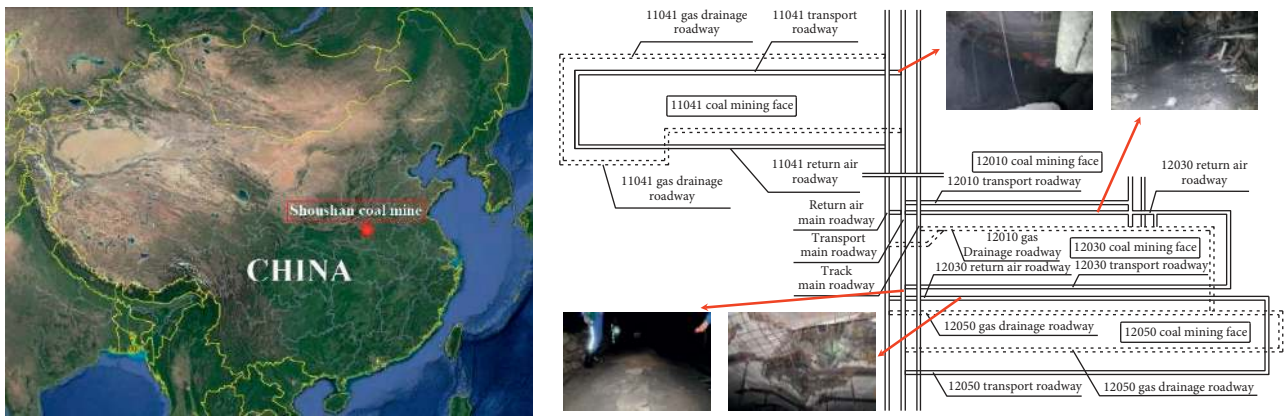

(a) (b)

Figure 1: (a) Location of coal mine; (b) the deformation and fracture situation of the roadway.

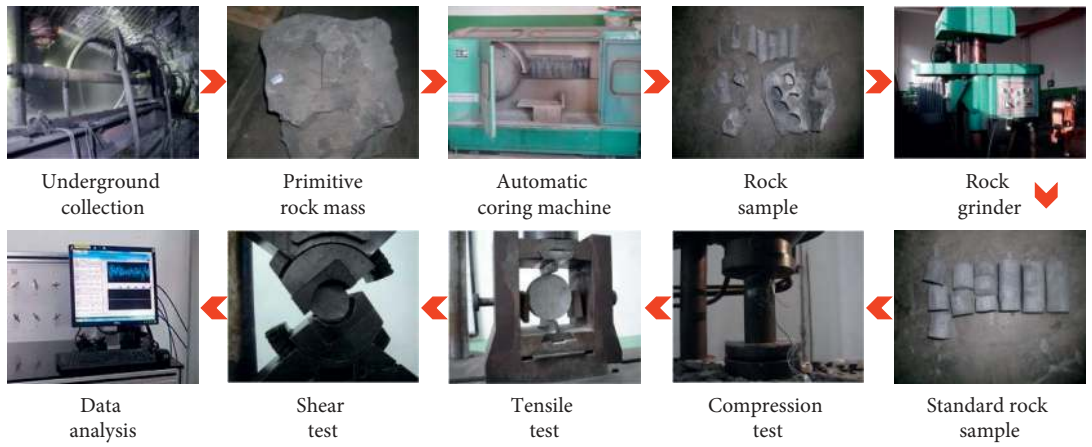

Figure 2: The experimental process.

Table 1: The physical and mechanical properties of roadway surrounding rock.

Lithology	Bulk density ($kN \cdot m^{-3}$)	Thickness (m)	Compressive strength (MPa)	Elastic modulus (GPa)	Poisson ratio	Interfriction angle (°)	Cohesion(MPa)	Tensile strength (MPa)
Fine sandstone	27.5	32	25.7	10.0	0.20	40	6.0	6.0
Sandy mudstone	25.3	8.0	9.4	3.5	0.22	34	2.5	2.5
No. 15 coal seam	13.6	3.5	4.2	2.5	0.25	19	1.5	1.5
Mudstone	24.5	3.5	7.2	2.5	0.23	32	2.0	2.0
No. 16 coal seam	13.6	6.5	4.7	2.0	0.23	32	1.5	1.4
Fine sandstone	27.5	5.0	25.7	10.0	0.20	40	6.0	6.0
Sandy mudstone	25.3	12	9.4	4.5	0.22	34	5.0	3.2
Limestone	28.0	13	30	10.0	0.20	40	8.0	7.2

remnant tectonic stress field is ubiquitous in deep rock mass, while the superposition and accumulation of them forms high stress; the ground stress of deep rock mass possesses obvious directivity, and especially that its horizontal stress is largely influenced by geologic structure. The ground stress measured data of mine indicate that horizontal stress is larger than vertical stress, and the specific value of maximum horizontal stress and vertical stress is 0.96–2.07; under the

function of high stress, the deep rock mass converts from fragility to ductility, which shows strong rheological behavior with large deformation and obvious "time effect." In addition, high ground temperature and high water pressure also produce prominent influence on correlated characteristic of rock mass.

3.2. Excavation Disturbance. Roadway excavation changes the mechanical state of the surrounding rock, and it possesses pressure relief function to the unexcavated rock. Deviator stress and sharp release of energy caused by excavation under high ground stress condition are the basic reasons of inducing the unstability of the deep roadway, and the main forms of the surrounding rock destruction are tension crack and shear failure. Destruction is a progressive process, and the strength of the surrounding rock is weakening continuously. Under the condition without support or with small support force, the destruction of the deep roadway presents specific regional fracture phenomenon, while, under the function of strong external support, the shear slip deformation inside the surrounding rock plays a dominant role.

3.3. Support Means. Bolt support is a kind of support method widely used by coal mine. Its function mainly is reflected in the destruction period of rock, but as for rock, which has entered into yield state, small supporting resistance even can improve its residual strength remarkably and make it be capable of bearing large load. The deformation amount and speed of the roadway increases clearly after it enters deep mining. Although the deformation and fracture of rock mass is unavoidable, bolt can provide certain constraining force to prevent the rock mass from sliding. Take the advantage of horizontal stress to maintain the roof stability by installing bolt and exerting high pretightening force timely, so as to allow roof to keep in horizontal compression state and enhance the stability of the roadway.

4. Theoretical Calculation of Stabilization Mechanism of the Deep Roadway

The stability of the deep roadway in different places is different when it is under the function of high ground stress,

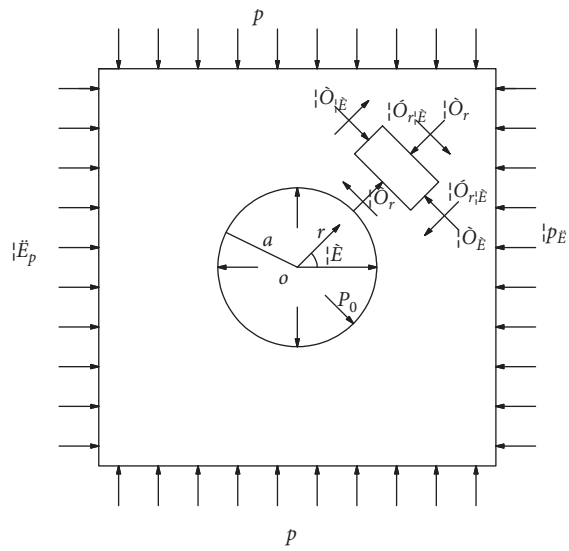

Figure 3: Mechanical model of the roadway.

and its mechanical characteristic shows that different places have different scopes of the plastic zone. Therefore, it needs to adopt the scope of the plastic zone as the evaluation index of the stability to make an analysis to the roadway stability state.

4.1. Model Establishment. The mechanical model of the roadway is shown in Figure 3. Former calculation of the plastic zone of the roadway is based on hydrostatic pressure state, while our research takes into consideration the influences of horizontal stress and supporting intensity on the roadway stability. According to the characteristics of deep stress field, it makes the following hypotheses: (1) rock mass is continuous, homogeneous, and isotropous elastic-plastic material; (2) the horizontal stress born by the roadway is λ times of vertical stress; (3) neglect the influence of dead load of the surrounding rock; and (4) the plastic zone of rock mass satisfies Mohr–Coulomb strength criterion.

4.2. Calculation of the Plastic Zone Scope. Surrounding rock stress formula of the round roadway in the elasticity zone [41]:

$$\left.\begin{aligned}
\sigma_r &= \frac{(1+\lambda)p}{2}\left(1-\frac{a^2}{r^2}\right)-\frac{(1+\lambda)p}{2}\left(1-\left(\frac{4a^2}{r^2}\right)+\left(\frac{3a^4}{r^4}\right)\right)\cos 2\theta+\frac{p_0a^2}{r^2},\\
\sigma_\theta &= \frac{(1+\lambda)p}{2}\left(1+\frac{a^2}{r^2}\right)+\frac{(1-\lambda)p}{2}\left(1+\frac{3a^4}{r^4}\right)\cos 2\theta-\left(\frac{p_0a^2}{r^2}\right),\\
\tau_{r\theta} &= \frac{(1-\lambda)p}{2}\left(1+\left(\frac{2a^2}{r^2}\right)-\left(\frac{3a^4}{r^4}\right)\right)\sin 2\theta,
\end{aligned}\right\} \quad (1)$$

where λ is the side pressure coefficient; p is the vertical stress, MPa; a is the radius of the roadway, m; r is the distance to the center of the roadway, m; P_0 is the supporting intensity, MPa; θ is the included angle with x-axis, °; σ_r is the radial direction normal stress, MPa; σ_θ is the tangential normal stress, MPa; and τr_θ is the shear stress, MPa.

One point's radial direction normal stress, tangential normal stress, and shear stress are known, and then, the principal stress of this point can be acquired by

$$\left.\begin{aligned}\sigma_1 &= \left(\frac{\sigma_r+\sigma_\theta}{2}\right)+\sqrt{\left(\frac{\sigma_r-\sigma_\theta}{2}\right)^2+\tau_{r\theta}^2},\\ \sigma_2 &= \frac{\sigma_r+\sigma_\theta}{2}-\sqrt{\left(\frac{\sigma_r-\sigma_\theta}{2}\right)^2+\tau_{r\theta}^2},\end{aligned}\right\} \tag{2}$$

where σ_1 is the maximum principal stress; and σ_2 is the minimum principal stress.

Substitute equation (1) into (2), and then, the principal stress of the surrounding rock of the round roadway in the elasticity zone can be acquired:

$$\left.\begin{aligned}\sigma_1 &= \frac{(1+\lambda)p}{2}-(\lambda-1)\left(\frac{pa^2}{r^2}\right)\cos 2\theta+\left(\frac{p}{2}\right)\beta,\\ \sigma_2 &= \frac{(1+\lambda)p}{2}-(\lambda-1)\left(\frac{pa^2}{r^2}\right)\cos 2\theta-\left(\frac{p}{2}\right)\beta.\end{aligned}\right\} \tag{3}$$

In the equation

$$\beta=\sqrt{\left[(1+\lambda)\left(\frac{a^2}{r^2}\right)-(\lambda-1)\left(1-\left(\frac{2a^2}{r^2}\right)+\left(\frac{3a^4}{r^4}\right)\right)\cos 2\theta-\left(\frac{2p_0a^2}{pr^2}\right)\right]^2+\left[(\lambda-1)\left(1+\left(\frac{2a^2}{r^2}\right)-\left(\frac{3a^4}{r^4}\right)\right)\sin 2\theta\right]^2}. \tag{4}$$

The principal stress of the point inside the plastic zone can be known by Mohr–Coulomb strength criterion:

$$\sigma_1=\left(\frac{1+\sin\phi}{1-\sin\phi}\right)\sigma_2+\left(\frac{2C\cos\phi}{1-\sin\phi}\right), \tag{5}$$

where C is the cohesion; and φ is the internal friction angle, °.

Substituting equation (3) into (5), the scope of the plastic zone of the surrounding rock of the round roadway in deep complex stress field can be acquired:

$$\left[(1+\lambda)q-2(\lambda-1)\left(\frac{qa^2}{r^2}\right)\cos 2\theta\right]\sin\phi-q\beta+2C\cos\phi=0. \tag{6}$$

The point (r,θ) satisfying with equation (6) locates at the boundary of the elastic zone and plastic zone, and the zone inside the boundary line is the plastic zone.

4.3. Influence Factors of the Plastic Zone Scope

4.3.1. Side Pressure Coefficient λ. Hypothesize vertical pressure q = 15 MPa, rock mass cohesion c = 1.5 MPa, internal friction angle $\varphi = 20°$, and support intensity P_0 = 0.3 MPa. When side pressure coefficient λ = 0.5, 1, 1.5, and 2, the distribution range of the plastic zone can be obtained as shown in Figure 4.

It can be inferred from Figure 4 that when λ is relatively small, the plastic zone of the roadway presents symmetric distribution, and the plastic destruction scope is about 1.0 m–3.0 m; when λ increases from 0.5 to 1.5, the scope of plastic zones at two sides of the roadway is decreasing gradually from 1.24 m to 0.73 m, and the scope of roof and floor plastic zones is increasing gradually from 0.29 m to 1.34 m; when λ is greater than 1.5, the scope of the plastic zone of the roadway increases rapidly, and the increase of humeral angle part is extremely remarkable; the scope of the plastic zone reaches to 3.47 m when $\lambda = 2$, which increases 160% than $\lambda = 1.5$, the value of λ at this time is the limit value of the roadway stability. It fully reflects the impact of horizontal stress on the stability of roof and floor of the roadway. When side pressure coefficient is greater than this value, the stability of the roadway will decreases rapidly, which coincides with a large number of field observation.

4.3.2. Vertical Pressure q. Hypothesize side pressure coefficient $\lambda = 2$, rock mass cohesion C 1.5 MPa, internal friction angle $\varphi = 20°$, and supporting intensity P_0 = 0.3 MPa. When vertical pressure q = 5, 10, 15, 20 MPa, the distribution range of the plastic zone of the roadway can be as shown in Figure 5.

It can be indicated from Figure 5 that with the increase of the burial depth of the roadway, the plastic zone is expanding constantly, and especially the diffusion from the humeral angle of the roadway towards the two sides is obvious. When vertical stress is relatively small (q < 5 MPa), the plastic fracture scope is less than 1.1 m, and the roadway is apt to stability at this time, but the expansion rate of the scope of the plastic zone is fast; after it enters deep part (q > 15 MPa), the scope of plastic fracture is more than 3.47 m, and it is difficult to keep the stability of the roadway, and the expansion rate of the plastic zone slows down.

4.3.3. Support Means. Hypothesize side pressure coefficient $\lambda = 2$, vertical pressure q = 15 MPa, rock mass cohesion C = 1.5 MPa, and internal friction angle $\varphi = 20°$; when supporting intensity P_0 = 0, 0.1, 0.2, 0.3, 0.4, 0.5 MPa, the

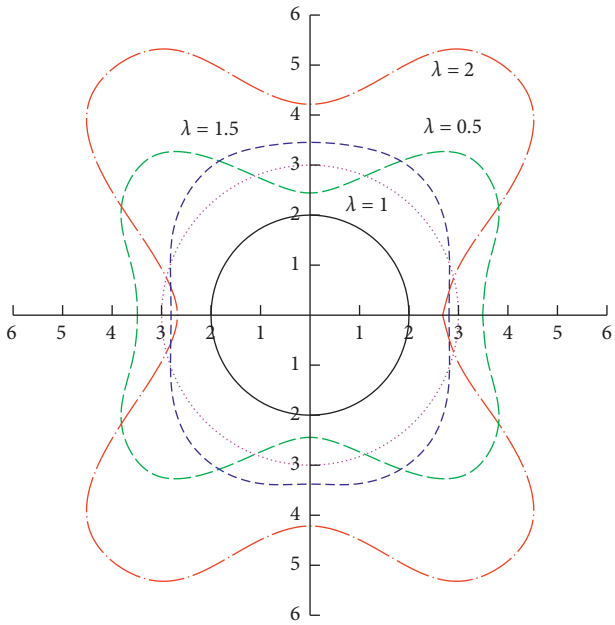

Figure 4: The distribution range of the plastic zone with different side pressure coefficients.

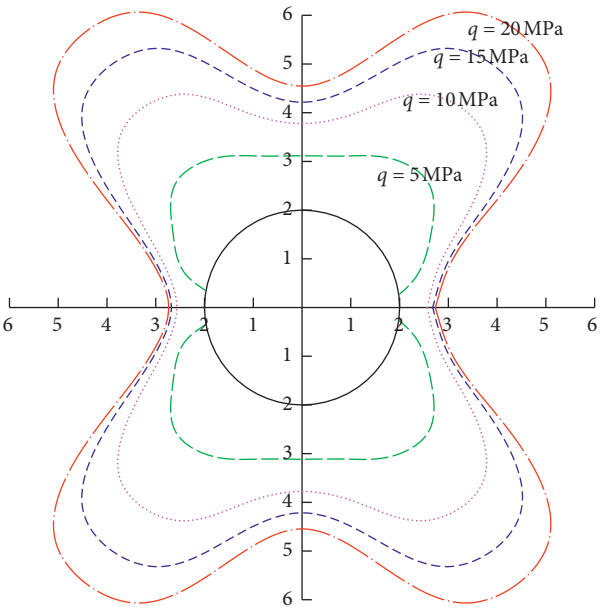

Figure 5: The distribution range of the plastic zone with different vertical pressure.

distribution range of the plastic zone can be as shown in Figure 6.

It can be inferred from Figure 6 that with the increase of support intensity p_0, the scope of the plastic zone L basically presents linear decrease. The linear relation is given as

$$L = 5.486 - 0.055p_0. \quad (7)$$

Although the function of bolt support to the decrease of the scope of the plastic zone is not obvious, it effectively

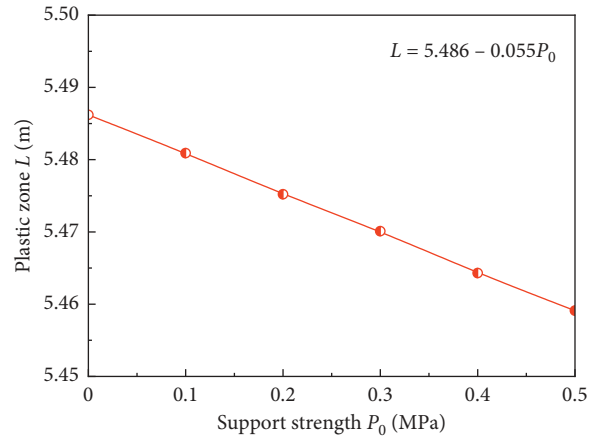

Figure 6: The plastic zone with different support intensity.

improves the residual strength of surrounding rock after peak [42] and restricts the further expansion of the plastic zone.

In summary, with the increase of ground stress, the stability of the roadway is becoming worse and worse; the influence of ground stress on the stability of the roadway is ununiform, that is, to say that the vertical stress mainly influences the stability of the two sides of the roadway, and the horizontal stress mainly influences the stability of roof and floor of the roadway.

5. Numerical Modeling of the Stabilization Mechanism of the Deep Roadway

5.1. Model Establishment. Taking the roadway of the 15# coal seam in Shoushan coal mine as an example, the numerical calculation model is established by making use of FLAC3D software. It makes a research on distribution and evolution rules with the stress, displacement, and the plastic zone and the influences of different intensities of horizontal stress it have on above factors. What is more, the size of the model is length × width × height = 180 m × 80 m × 83.5 m, the total number of unit is 321600, and the total number of node is 337348. The sides of this model are restricted horizontal mobility, its underside is restricted vertical shift, and its upper surface is stress boundary. Impose 15 MPa to simulate the dead weight of overlying rock mass, and the material conforms to the Mohr–Coulomb model. The numerical calculation model is shown in Figure 7. The research contents are (1) the distribution and evolution rules of stress, displacement, and the plastic zone of the roadway; (2) the influences of horizontal stress on the stability of the roadway; and (3) the function of bolt support on the deep roadway.

5.2. Distribution and Evolution Rules of Stress, Displacement, and the Plastic Zone of the Deep Roadway

5.2.1. Evolution Rule of Vertical Stress. After the excavation of the roadway, the two sides form the stress concentration zone, and the stress concentration factor increases from 1.20

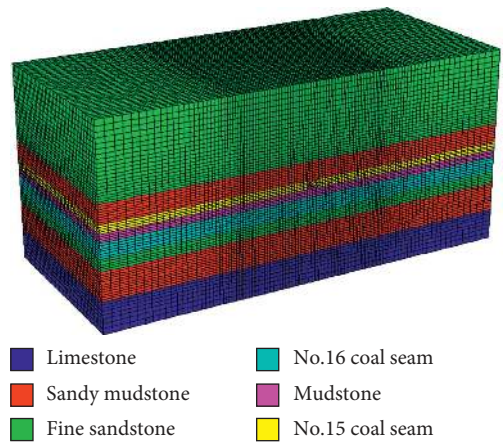

Figure 7: Numerical calculation model.

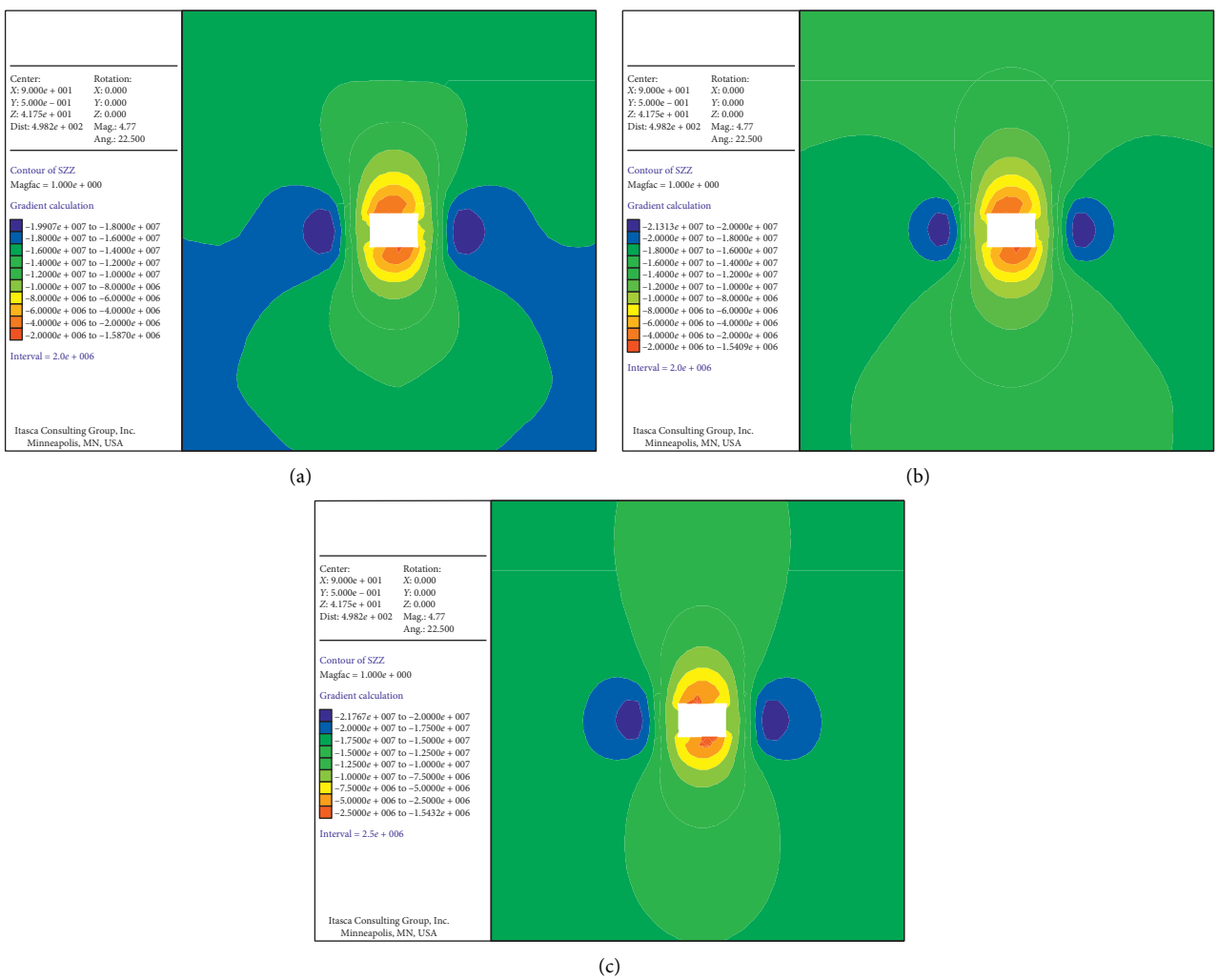

Figure 8: Cloud diagram of vertical stress. (a) 300 step; (b) 600 step; and (c) 2100 step.

to 1.43; the surrounding rock in certain scope of the roadway is relatively broken and forms the stress decreasing zone. After the roadway deformation tends to be stable, the stress decreasing zone presents "bowling-form" distribution at roof and floor, and the scope is relatively large. The cloud diagram of vertical stress is shown in Figure 8.

5.2.2. Distribution and Evolution Rule of Horizontal Stress. After the excavation of the roadway, the two sides appear as large scope of the stress decreasing zone, and the floor emerges as small scope of the stress concentration zone. During the stability process of the roadway, the stress concentration zone of roof and floor is enlarging constantly, and especially in the floor of the roadway whose stress concentration zone is relatively large. Moreover, the stress distribution of the two sides is basically invariant. The cloud diagram of horizontal stress is shown in Figure 9.

5.2.3. Distribution and Evolution Rule of Shear Stress. After the excavation of the roadway, with the increase of deviator stress $\sigma_1 - \sigma_3$, it forms the shear stress concentration zone at the four corners of the roadway. It can be known from shear stress mutual equal theory that shear stress comes in pairs, the directions of shear stress of adjacent two surfaces is opposite, and the intensity of shear stress is 6.0 MPa after the stability of the roadway. The cloud diagram of shear stress is shown in Figure 10.

5.2.4. Distribution and Evolution Rule of Displacement. After the excavation of the roadway, the surrounding rock moves towards excavation direction. Due to that the vertical stress forms the stress concentration zone at the two sides, so the coal of the two sides bear great pressure, while the strength of coal is relatively low, so the displacement of the two sides is large. The cloud diagram of displacement is shown in Figure 11.

5.2.5. Distribution and Evolution Rule of the Plastic Zone. After excavation of the roadway, stress concentration area appears in roof and floor. Shear failure is serious, and the two sides present small scope of tensile failure. The destruction of the roadway is mainly shear failure, and it presents small scope of the tensile-shear mixed fracture zone at the center of roof and the middle part of the two sides. The cloud diagram of the plastic zone is shown in Figure 12.

In conclusion, the two sides form the stress concentration zone under the function of vertical stress in deep stress field after the excavation of the roadway; furthermore, the roof and floor show large scope of the stress decreasing zone; under the function of horizontal stress, it appears in large scope of the horizontal stress concentration zone at the roof and floor, and the side angle appears in the shear stress concentration zone, so the roof and floor rock masses are easy to occur as shear failure. Therefore, under the function of deep high stress, the key to stabilize the deep roadway is to improve the rigidity and strength of roof and floor rock masses, and especially the important load bearing parts of vertex angle and side angle.

5.3. Horizontal Stress Action Mechanism. One of the prominent characteristics of deep ground stress is that horizontal stress is higher than vertical stress [43]. The ground stress testing results of this coal mine show that the specific value of maximum horizontal stress and vertical stress is 0.96–2.07. Therefore, the value range of side pressure coefficient selected in numerical calculation is 1-2.

5.3.1. Displacement Distribution of the Roadway

(1) The displacement of the roadway basically presents positive exponential distribution with the enlarging of distance from the roadway surface; furthermore, the horizontal displacement of the two sides keeps stable when its distance to the two sides is 4.0 m, the vertical displacement of floor keeps stable when its distance to the floor is 7.0 m, and the vertical displacement of roof keeps stable when its distance to the roof is 7.0 m.

(2) With the increase of side pressure coefficient, the surface displacement of the roadway increases constantly. The influence of horizontal stress on the stability of the roadway exists obvious boundary. In addition, when the side pressure coefficient is larger than 1.2, the roadway loses stability rapidly.

(3) The increase of horizontal stress has a great influence on the roof and floor, while it has a small influence on the two sides. The displacement distribution of the roadway is shown in Figure 13.

5.3.2. Stress Distribution of the Roadway

(1) As the distance from the roadway surface is farther, the vertical stress of the two sides first increases and then decreases; moreover, the peak stress appears at the place of 5.0 m, and the stress tends to be stable after 10 m. The horizontal stress of the two sides is increasing constantly, and there is no obvious peak value; the vertical stress of roof and floor increases constantly without obvious peak value. The horizontal stress of roof and floor first increases and then decreases, and there is a certain fluctuation in the scope of 10 m of roof and floor, and the horizontal stress gradually tends to be stable after 15 m.

(2) With the increase of side pressure coefficient, the distribution and intensity of vertical stress of two sides keep unchanged basically with small influence of horizontal stress; the vertical stress distribution of roof and floor gradually transits from "arc-shape" distribution to "ellipse shape," and the vertical stress is increasing constantly. The stress distribution of the roadway is shown in Figure 14.

5.3.3. Plastic Zone Distribution of the Roadway. With the increase of side pressure coefficient, the failure mode of the roadway keeps unchanged, which is mainly shear failure and shear-tensile failure. But, the coverage area of shear-tensile failure to the area of the roadway failure is decreasing continuously, and the scope of shear failure is increasing constantly, so horizontal stress intensifies the shear failure of the roadway. The plastic zone distribution of the roadway is shown in Figure 15.

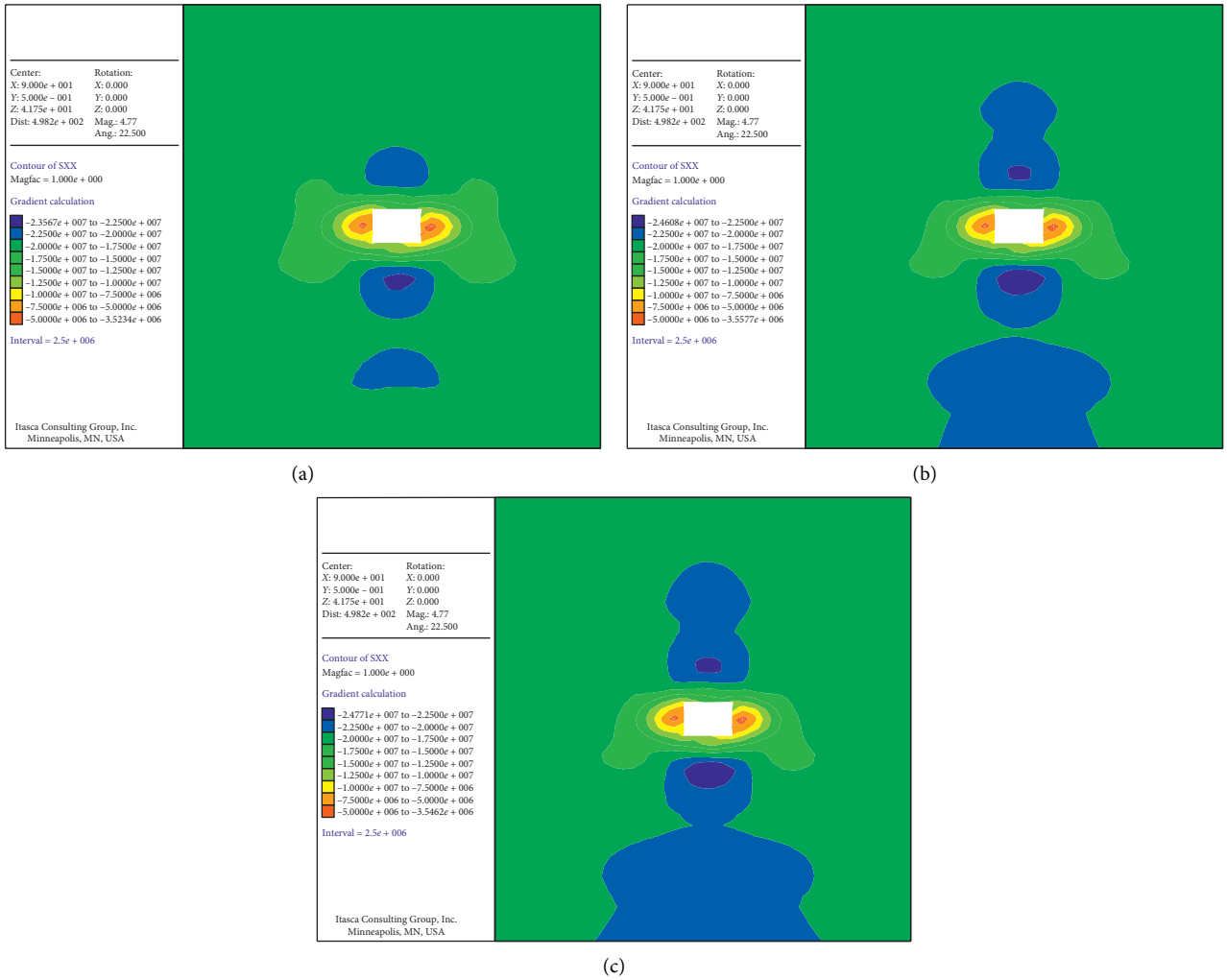

Figure 9: Cloud diagram of horizontal stress. (a) 300 step; (b) 600 step; and (c) 2100 step.

6. Bolt Support Mechanism for the Deep Roadway

As for the interaction relation between bolt and surrounding rock, scholars made large amount of research studies on the amelioration of mechanical property of rock mass after bolt strengthening, which revealed the mechanism of bolt support in different degrees. However, these achievements mainly come from shallow-buried tunnel engineering, and its research emphasis is the anchoring effect of unbroken rock and soil mass. While, under the influence of high stress and strong mining, the surrounding rock of the deep roadway especially the coal roadway occurs as large deformation and large scope of destruction; therefore, it needs to make a further study on bolt support mechanism under such condition. The bolt support structure of the roadway is shown in Figure 16. There are six bolts at roof, four bolts at each side of the two sides, row spacing is 800 mm, interspacing of anchor is 3000 mm, and row spacing of anchor is 1600 mm.

6.1. Roadway Deformation. Under the condition of with or without support, the horizontal displacement difference of the two sides is enlarging constantly when it transits from the deep of surrounding rock towards the surface of the roadway, but the maximum displacement difference is just 24 mm, and the vertical displacement of roof and floor keeps unchanged generally. Although bolt support improves the parameters of shallow surrounding rock's internal friction angle and cohesive force, the shallow surrounding rock stress of the deep roadway is still very high, and the effect of bolt support is not significant. The horizontal displacement of the two sides of the roadway is shown in Figure 17.

6.2. Roadway Stress. Compared with the condition without support, under the function of bolt support, the stress intensity and distribution rule of the roadway have no big changes. Due to that the scope of the horizontal stress decreasing zone of the two sides is large, and the stress environment is good, so the effect of bolt support of the two

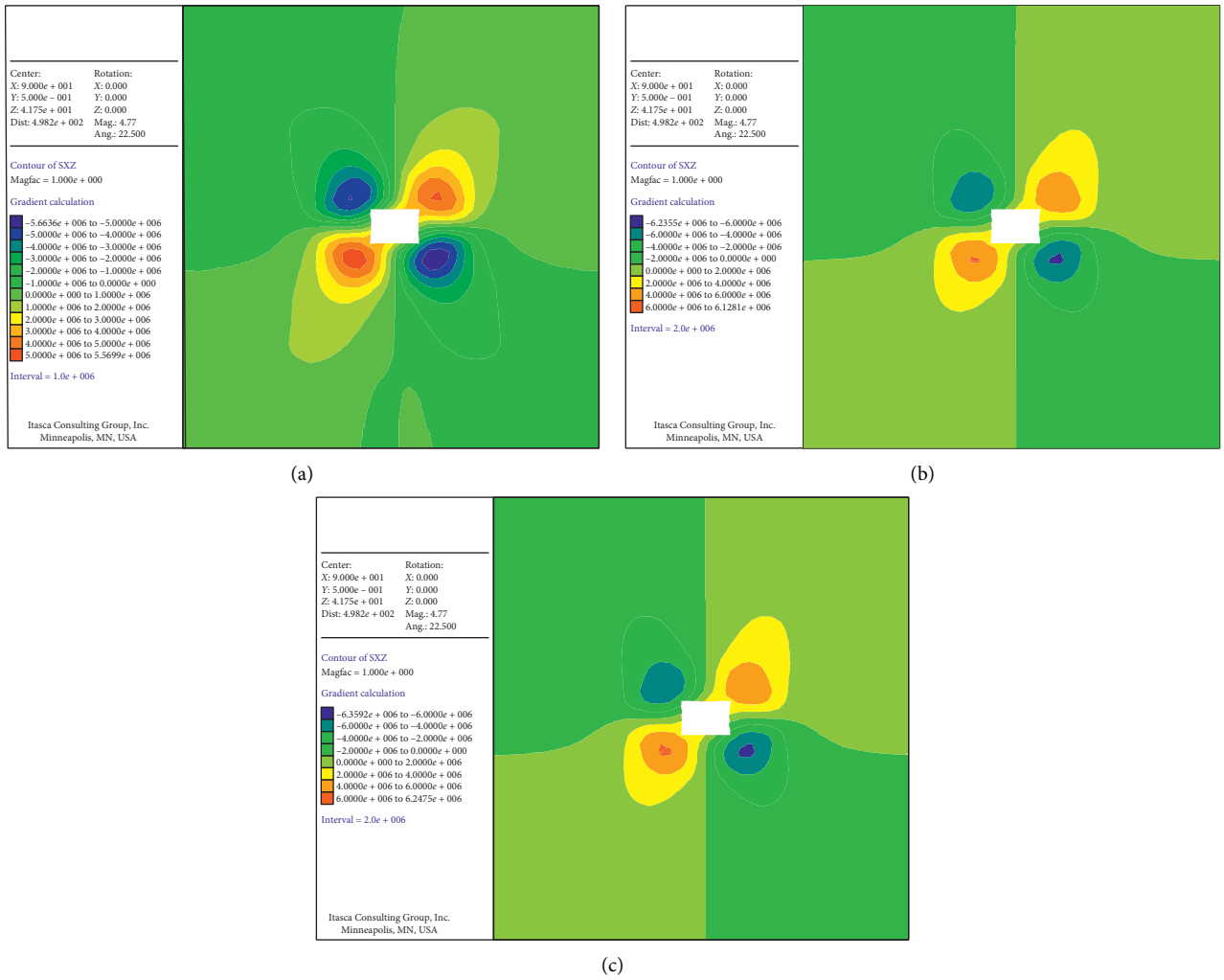

Figure 10: Cloud diagram of shear stress. (a) 300 step; (b) 600 step; and (c) 2100 step.

sides is more remarkable than that of roof. In addition, bolt support improves the confining pressure of the surface of the roadway, and the increase of confining pressure remarkably decreases the deformation of the roadway, on account of that the shallow surrounding rock of the roadway is mellow and broken, and it is sensitive to confining pressure. The cloud diagram of the roadway stress is shown in Figure 18.

6.3. Roadway Failure. Compared with the condition without support, the scope of the plastic zone of the roadway decreases to some extent under the function of bolt. When there is no support, the surrounding rock in the middle part of the roadway mainly presents shear failure and tensile failure, while bolt support can effectively decrease the scope of tensile failure of the surface of the roadway, and the destruction range of roof can decrease from 3 m without support to 1 m with support, so bolt support can strengthen the stability of the roadway. The cloud diagram of the plastic zone is shown in Figure 19.

6.4. Bolt Stress. The bolt of the roadway bears the dilatation deformation stress of the surrounding rock as it restrains the surrounding rock, so it keeps in tension state. The axial force of bolt reaches to maximum at the middle part of two sides, that of the middle part of roof takes second place, and that of vertex angle is minimum; moreover, the maximum axial force of bolt is 200 kN, and the minimum axial force of bolt is 147 kN. The maximum axial force of anchor is 304.2 kN. The bolt has entered into yield state as for bolt with BHRB335 texture and diameter of 20 mm, and the anchor also has entered into yield state as for anchor with a diameter of 15.24 mm. The force diagram of bolt and anchor is shown in Figure 20.

In conclusion, when the shallow surrounding rock stress of the roadway is relatively low, ordinary bolt support has a good effect on surrounding control, but the deformation of the roadway has not yet received an effective control on the whole, both bolt and anchor bear great tension and enter into yield state, and the supporting structure approaches destruction. Therefore, in order to

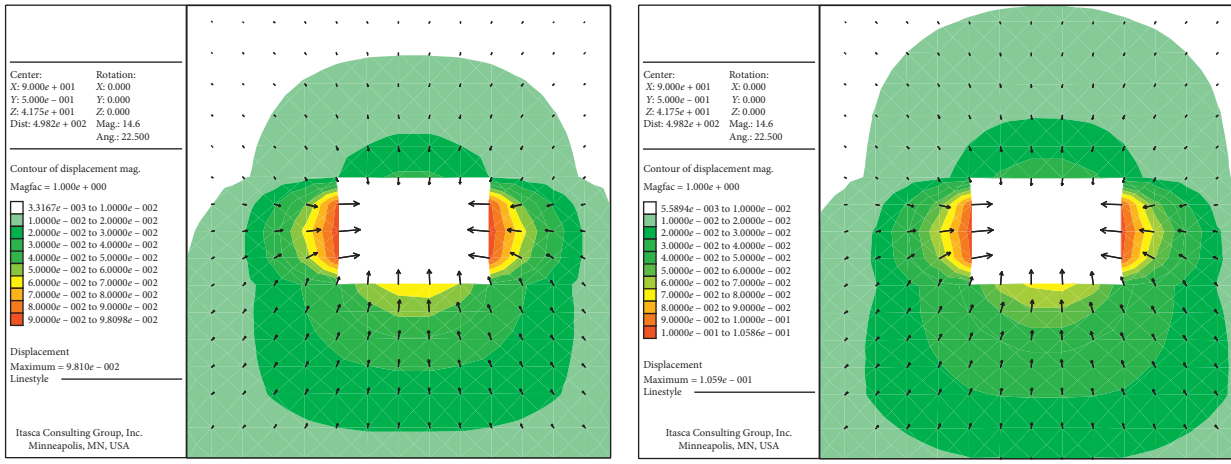

Figure 11: Cloud diagram of displacement. (a) 300 step; (b) 600 step; and (c) 2100 step.

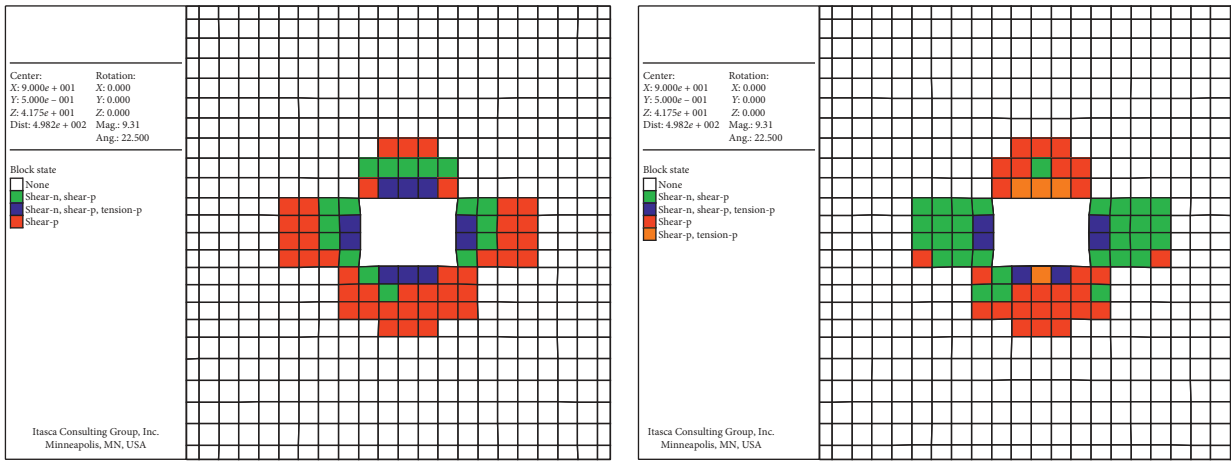

Figure 12: Continued.

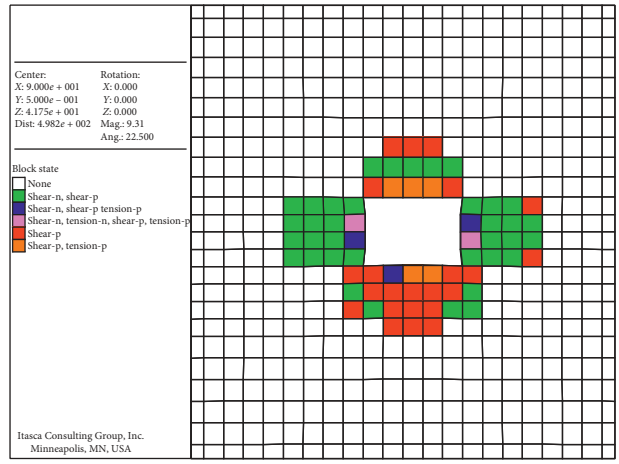

(c)

Figure 12: Cloud diagram of the plastic zone. (a) 300 step; (b) 600 step; and (c) 2100 step.

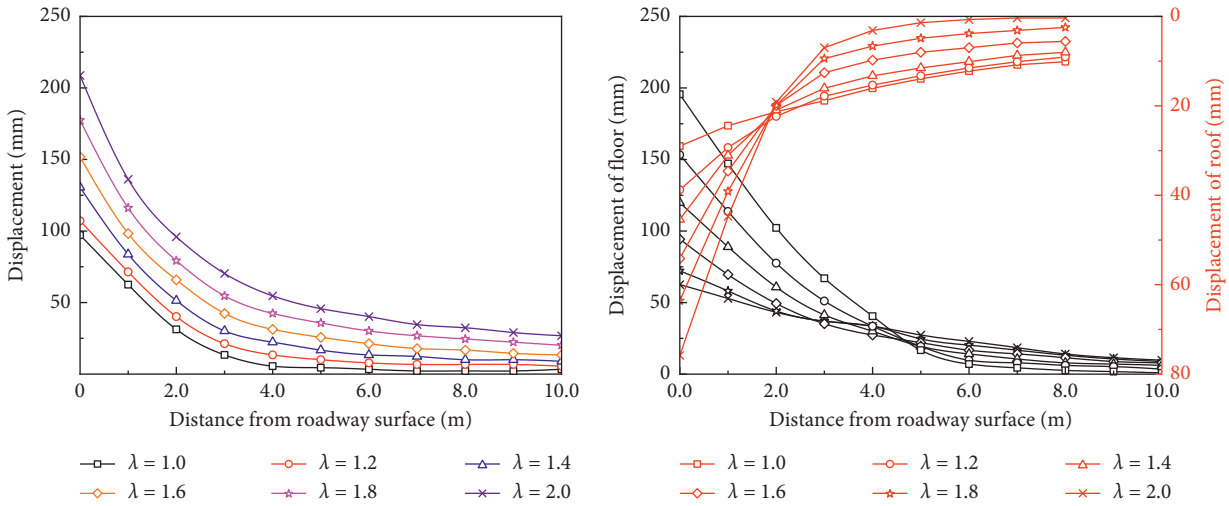

(a) (b)

Figure 13: The displacement distribution of the roadway. (a) Two sides; (b) roof and floor.

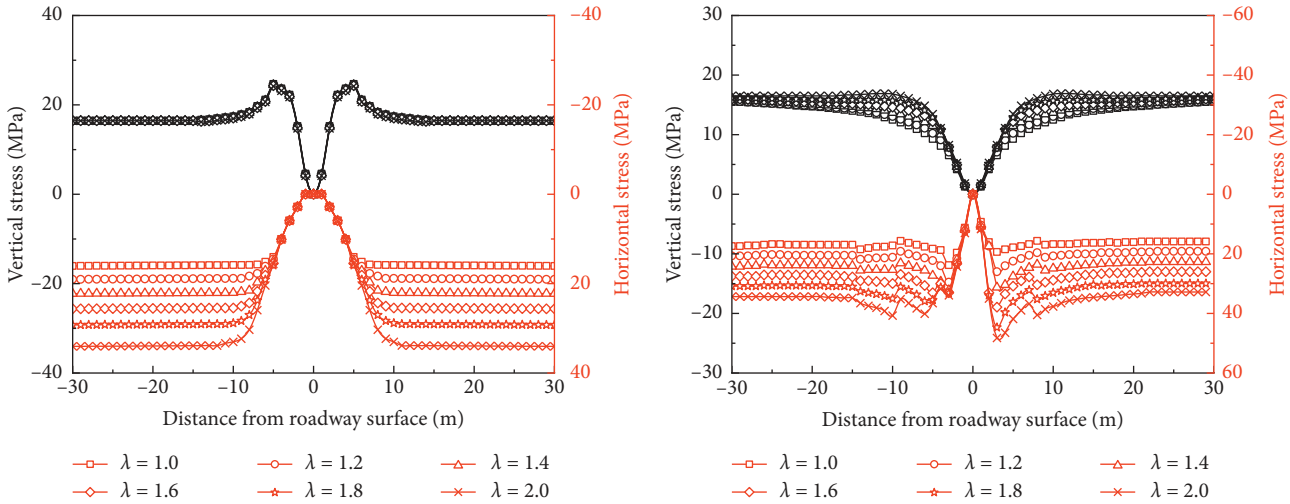

(a) (b)

Figure 14: The stress distribution of the roadway. (a) Two sides; (b) roof and floor.

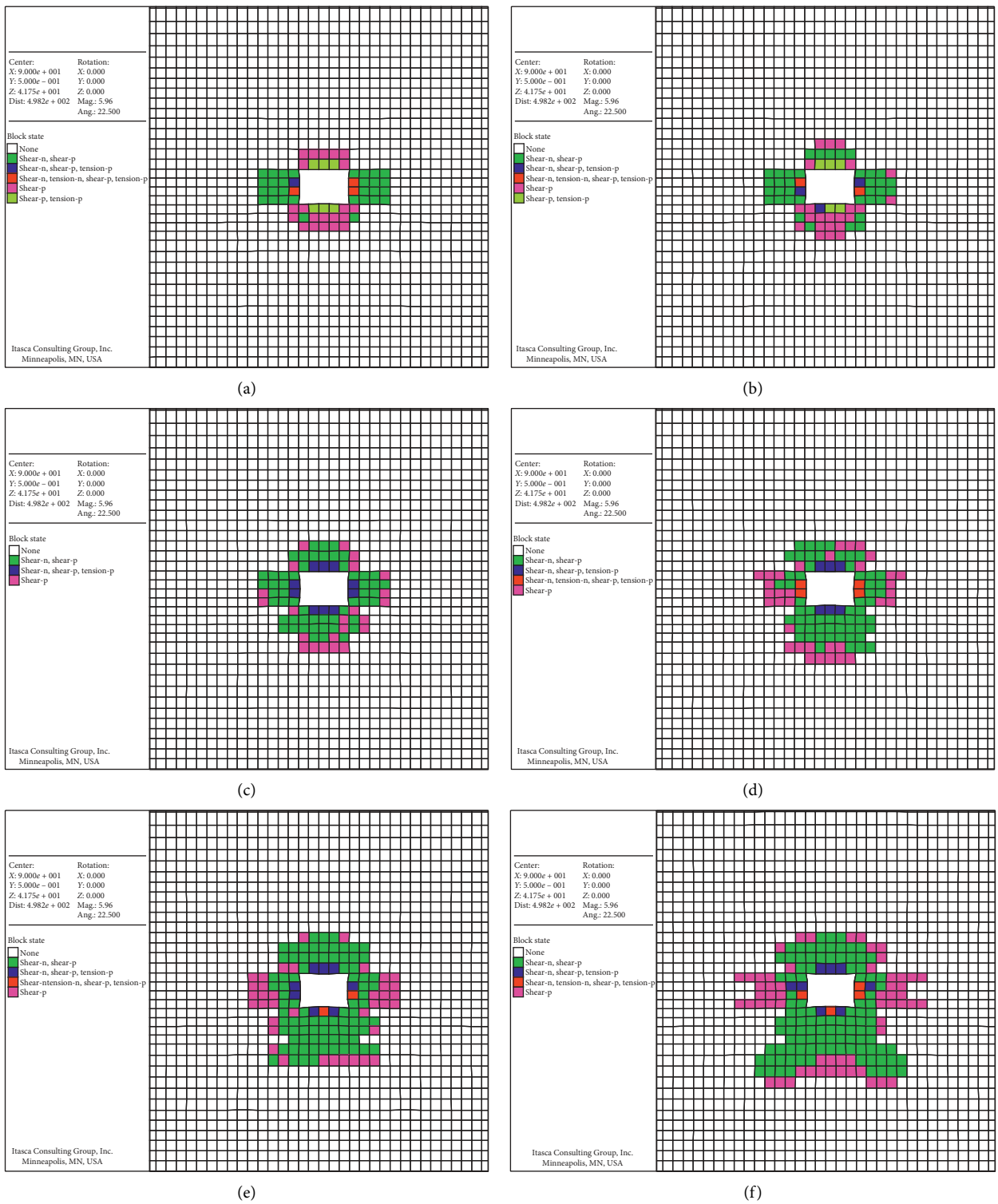

Figure 15: The plastic zone distribution of the roadway. (a) $\lambda = 1.0$; (b) $\lambda = 1.2$; (c) $\lambda = 1.4$; (d) $\lambda = 1.6$; (e) $\lambda = 1.8$; and (f) $\lambda = 2.0$.

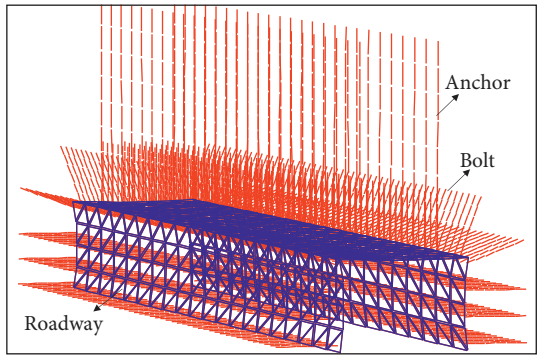

Figure 16: The bolt support structure of the roadway.

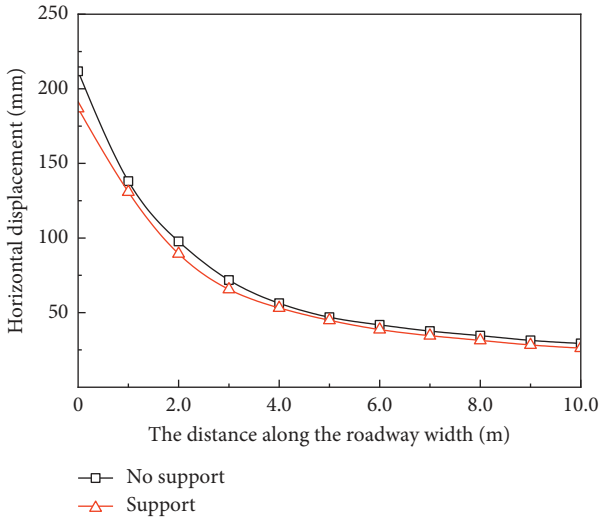

Figure 17: The horizontal displacement of the two sides of the roadway.

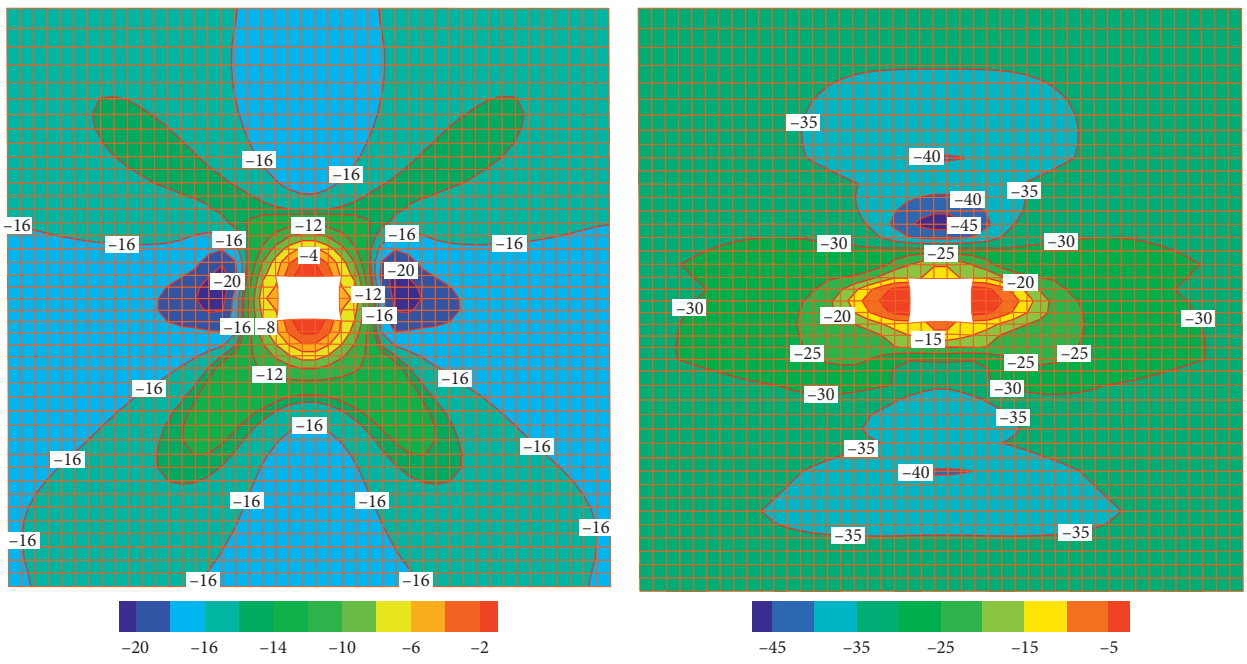

Figure 18: Continued.

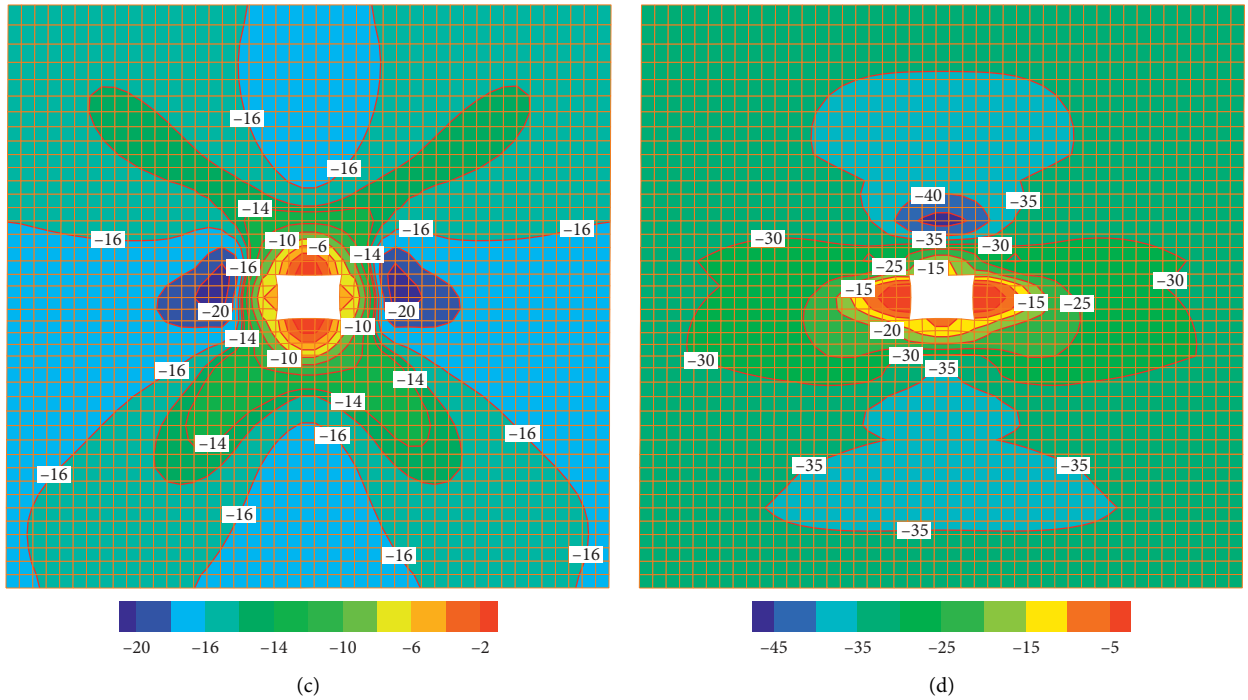

Figure 18: Cloud diagram of the roadway stress. (a) Vertical stress with no support; (b) horizontal stress with no support; (c) vertical stress with support; and (d) horizontal stress with support.

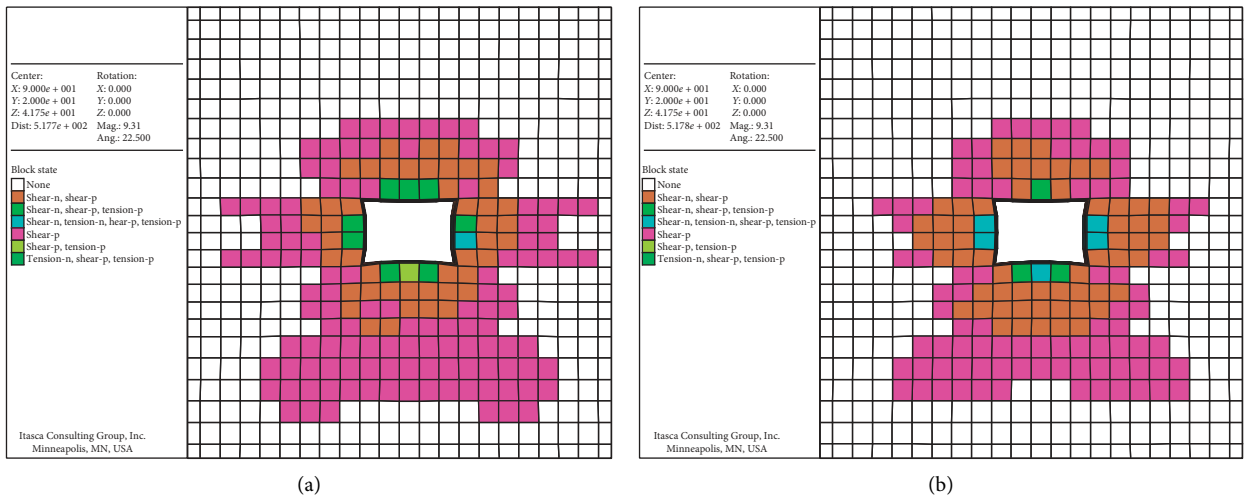

Figure 19: Cloud diagram of the plastic zone. (a) No support; (b) support.

ensure the stability of the deep roadway, it needs to adopt a high-strength anchor to make the surrounding rock depressurization on the basis of high support resistance, so as to adapt to the characteristics of large and sharp deformation of the deep roadway, and make the roadway be in low stress environment, which is easy to be maintained.

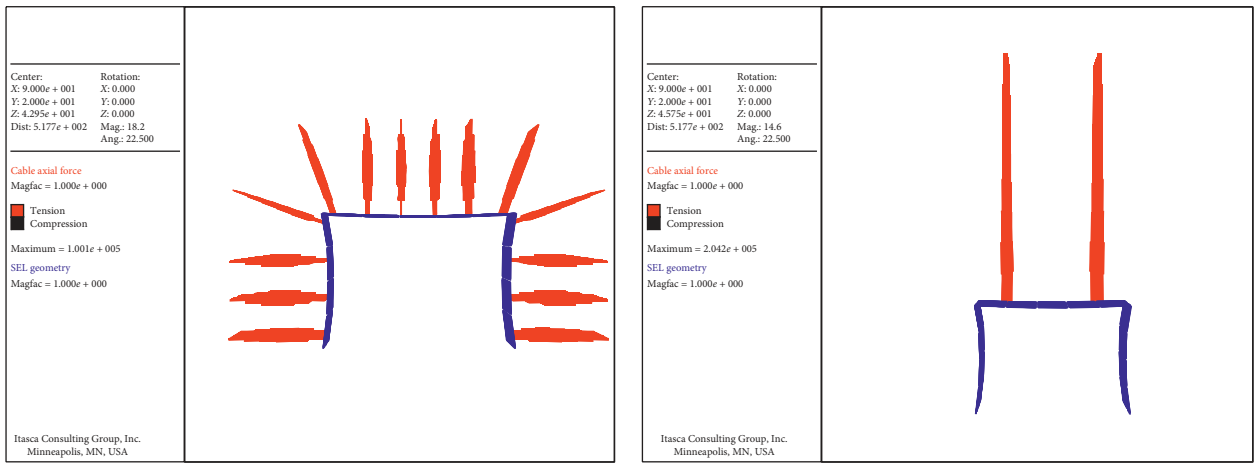

(a) (b)

Figure 20: The force diagram of bolt and anchor is shown. (a) Bolt; (b) anchor.

7. Conclusion

(1) The mechanical model of the deep roadway was established, and the theoretical calculation formula of the plastic zone of the roadway is obtained. With the increase of the vertical stress, the plastic zone is expanding constantly, and especially, the diffusion from the humeral angle of the roadway towards the two sides is obvious. While, with the increase of the horizontal stress, there is the limit value of the roadway stability. The support intensity to the decrease of the scope of the plastic zone is not obvious.

(2) The distribution and evolution rule of stress, displacement, and the plastic zone of the deep roadway was obtained. The two sides form the stress concentration zone under the function of vertical stress; furthermore, the roof and floor shows large scope of the stress decreasing zone. Under the function of horizontal stress, it appears large scope of the horizontal stress concentration zone at the roof nad floor, and it appears the shear stress concentration zone at the side angle and vertex angle of the roadway, so the roof and floor rock masses are easy to occur shear failure. Therefore, the key to stabilize the deep roadway is to improve the strength of the surrounding rock, and especially the important load bearing parts of vertex angle and side angle.

(3) With the increase of horizontal stress, the surrounding rock loses stability quickly. However, when at the same place, the vertical stress of roof and floor is increasing constantly, and the vertical stress of the two sides keeps unchanged basically, while the horizontal stress of roof and floor is increasing constantly, and so as that of the two sides. The plastic zone of the roadway expands sharply, and the proportion of shear failure is bigger and bigger. Therefore, it is extremely important to enhance the stability of the two sides and control the floor heave on the basis of ensuring the stability of roof.

(4) When the shallow surrounding rock stress of the roadway is relatively low, ordinary bolt support has a good effect on surrounding control, but the deformation of the roadway has not yet received an effective control on the whole, both bolt and anchor bear great tension and enter into yield state, and the supporting structure approaches destruction. Therefore, it needs to adopt a high-strength anchor to make surrounding rock depressurization on the basis of high support resistance.

Data Availability

No data were used to support this study.

Conflicts of Interest

The authors declare that they have no conflicts of interest.

Authors' Contributions

Dingchao Chen conceived and designed the research. Xiangyu Wang performed the numerical simulation and field tests. Lianying Zhang provided theoretical guidance in the research process. Yang Yu analyzed the data and wrote the paper.

Acknowledgments

This research was funded by the National Nature Science Foundation of China (grant numbers 51904269 and 51974269), the Fifth "333 Project" Scientific Research Project of Jiangsu, China, in 2019 (grant number BRA2019236), and the Outstanding Backbone Teachers of "Innovation Project" of University in JiangSu Province, China, in 2020, which are gratefully acknowledged.

References

[1] S. C. Li, Q. Wang, H. T. Wang et al., "Model test study on surrounding rock deformation and failure mechanisms of deep roadways with thick top coal," *Tunnelling and Underground Space Technology*, vol. 47, pp. 52–63, 2015.

[2] M. Chen, S.-Q. Yang, Y.-C. Zhang, and C.-W. Zang, "Analysis of the failure mechanism and support technology for the dongtan deep coal roadway," *Geomechanics and Engineering*, vol. 11, no. 3, pp. 401–420, 2016.

[3] R.-H. Cao, P. Cao, and H. Lin, "A kind of control technology for squeezing failure in deep roadways: a case study," *Geomatics, Natural Hazards and Risk*, vol. 8, no. 2, pp. 1715–1729, 2017.

[4] X.-R. Meng, R. Peng, G.-M. Zhao, and Y.-M. Li, "Roadway engineering mechanical properties and roadway structural instability mechanisms in deep wells," *KSCE Journal of Civil Engineering*, vol. 22, no. 5, pp. 1954–1966, 2017.

[5] Q. Wang, R. Pan, B. Jiang et al., "Study on failure mechanism of roadway with soft rock in deep coal mine and confined concrete support system," *Engineering Failure Analysis*, vol. 81, pp. 155–177, 2017.

[6] G. Xue, J. Cheng, J. Guan et al., "The method for determining working resistance of advance support bracket in deep fully mechanized roadway based on flac3d," *Advances in Mechanical Engineering*, vol. 10, no. 6, 2018.

[7] J. Zhang, L. Liu, J. Cao, X. Yan, and F. Zhang, "Mechanism and application of concrete-filled steel tubular support in deep and high stress roadway," *Construction and Building Materials*, vol. 186, pp. 233–246, 2018.

[8] F. Qi and Z. Ma, "Investigation of the roof presplitting and rock mass filling approach on controlling large deformations and coal bumps in deep high-stress roadways," *Latin American Journal of Solids and Structures*, vol. 16, no. 4, 2019.

[9] Z. Xiao, J. Liu, S. Gu et al., "A control method of rock burst for dynamic roadway floor in deep mining mine," *Shock and Vibration*, vol. 2019, Article ID 7938491, 16 pages, 2019.

[10] Z. Xie, N. Zhang, X. Feng, D. Liang, Q. Wei, and M. Weng, "Investigation on the evolution and control of surrounding rock fracture under different supporting conditions in deep roadway during excavation period," *International Journal of Rock Mechanics and Mining Sciences*, vol. 123, 2019.

[11] C. J. Hou, "Effective approach for surrounding rock control in deep roadway," *Journal of China University of Mining and Technology*, vol. 46, no. 3, pp. 467–473, 2017.

[12] R. Peng, X. Meng, G. Zhao, Y. Li, and J. Zhu, "Experimental research on the structural instability mechanism and the effect of multi-echelon support of deep roadways in a kilometre-deep well," *PLoS One*, vol. 13, no. 2, Article ID e0192470, 2018.

[13] J. Zhang, L. Liu, J. Shao, and Q. Li, "Mechanical properties and application of right-hand rolling-thread steel bolt in deep and high-stress roadway," *Metals*, vol. 9, no. 3, p. 346, 2019.

[14] H. P. Kang, J. H. Wang, and J. Lin, "High pretensioned stress and intensive bolting system and its application in deep roadways," *Journal of China Coal Society*, vol. 32, no. 12, pp. 1233–1238, 2007.

[15] Z. Liu, A. Cao, G. Zhu, and C. Wang, "Numerical simulation and engineering practice for optimal parameters of deep-hole blasting in sidewalls of roadway," *Arabian Journal for Science and Engineering*, vol. 42, no. 9, pp. 3809–3818, 2017.

[16] C.-L. Dong, G.-M. Zhao, X.-Y. Lu, X.-R. Meng, Y.-M. Li, and X. Cheng, "Similar simulation device for unloading effect of deep roadway excavation and its application," *Journal of Mountain Science*, vol. 15, no. 5, pp. 1115–1128, 2018.

[17] W. Zhang, Z. He, D. Zhang, D. Qi, and W. Zhang, "Surrounding rock deformation control of asymmetrical roadway in deep three-soft coal seam: a case study," *Journal of Geophysics and Engineering*, vol. 15, no. 5, pp. 1917–1928, 2018.

[18] M. C. He and Z. B. Guo, "Mechanical property and engineering application of anchor bolt with constant resistance and large deformation," *Chinese Journal of Rock Mechanics and Engineering*, vol. 33, no. 7, pp. 1297–1308, 2014.

[19] X.-M. Sun, F. Chen, M.-C. He, W.-L. Gong, H.-C. Xu, and H. Lu, "Physical modeling of floor heave for the deep-buried roadway excavated in ten degree inclined strata using infrared thermal imaging technology," *Tunnelling and Underground Space Technology*, vol. 63, pp. 228–243, 2017.

[20] J. B. Bai and C. J. Hou, "Control principle of surrounding rocks in deep roadway and its application," *Journal of China University of Mining and Technology*, vol. 35, no. 2, pp. 145–148, 2006.

[21] S.-Q. Yang, M. Chen, H.-W. Jing, K.-F. Chen, and B. Meng, "A case study on large deformation failure mechanism of deep soft rock roadway in xin'an coal mine, China," *Engineering Geology*, vol. 217, pp. 89–101, 2017.

[22] D. Wang, Y. Jiang, X. Sun, H. Luan, and H. Zhang, "Nonlinear large deformation mechanism and stability control of deep soft rock roadway: a case study in China," *Sustainability*, vol. 11, no. 22, 2019.

[23] W. J. Wang, C. Yuan, W. J. Yu et al., "Control technology of reserved surrounding rock deformation in deep roadway under high stress," *Journal of China Coal Society*, vol. 41, no. 9, pp. 2156–2164, 2016.

[24] X. Shengrong, G. Mingming, C. Dongdong et al., "Stability influence factors analysis and construction of a deep beam anchorage structure in roadway roof," *International Journal of Mining Science and Technology*, vol. 28, no. 3, pp. 445–451, 2018.

[25] S. C. Li, H. P. Wang, Q. H. Qian et al., "In-situ monitoring research on zonal disintegration of surrounding rock mass in deep mine roadways," *Chinese Journal of Rock Mechanics and Engineering*, vol. 27, no. 8, pp. 1545–1553, 2008.

[26] Q. S. Liu, C. B. Lu, B. Liu, and X. W. Liu, "Research on the grouting diffusion mechanism and its application of grouting reinforcement in deep roadway," *Journal of Mining and Safety Engineering*, vol. 31, pp. 333–339, 2014.

[27] W. P. Huang, Q. Yuan, Y. L. Tan et al., "An innovative support technology employing a concrete-filled steel tubular structure for a 1000 m-deep roadway in a high in situ stress field," *Tunnelling and Underground Space Technology*, vol. 73, pp. 26–36, 2018.

[28] C. Wang, L. Liu, D. Elmo et al., "Improved energy balance theory applied to roadway support design in deep mining," *Journal of Geophysics and Engineering*, vol. 15, no. 4, pp. 1588–1601, 2018.

[29] Y. Yuan, W. Wang, S. Li, and Y. Zhu, "Failure mechanism for surrounding rock of deep circular roadway in coal mine based on mining-induced plastic zone," *Advances in Civil Engineering*, vol. 2018, Article ID 1835381, 14 pages, 2018.

[30] J. C. Chang and G. X. Xie, "Mechanical characteristics and stability control of rock roadway surrounding rock in deep mine," *Journal of China Coal Society*, vol. 34, no. 7, pp. 881–886, 2009.

[31] Y. Cheng, J. Bai, Y. Ma, J. Sun, Y. Liang, and F. Jiang, "Control mechanism of rock burst in the floor of roadway driven along next goaf in thick coal seam with large obliquity angle in deep well," *Shock and Vibration*, vol. 2015, Article ID 750807, 10 pages, 2015.

[32] B. Jiang, L. Wang, Y. Lu, S. Gu, and X. Sun, "Failure mechanism analysis and support design for deep composite soft rock roadway: a case study of the yangcheng coal mine in China," *Shock and Vibration*, vol. 2015, Article ID 452479, 14 pages, 2015.

[33] J. K. Long, "The mechanism of synergetic anchorage in deep roadway surrounding rock," *Journal of Mining and Safety Engineering*, vol. 33, no. 1, pp. 19–26, 2016.

[34] J. Ning, J. Wang, Y. Tan, and X. Shi, "Dissipation of impact stress waves within the artificial blasting damage zone in the surrounding rocks of deep roadway," *Shock and Vibration*, vol. 2016, Article ID 4629254, 13 pages, 2016.

[35] R. Pan, Q. Wang, B. Jiang et al., "Failure of bolt support and experimental study on the parameters of bolt-grouting for supporting the roadways in deep coal seam," *Engineering Failure Analysis*, vol. 80, pp. 218–233, 2017.

[36] H. Zhang, X. Miao, G. Zhang, Y. Wu, and Y. Chen, "Non-destructive testing and pre-warning analysis on the quality of bolt support in deep roadways of mining districts," *International Journal of Mining Science and Technology*, vol. 27, no. 6, pp. 989–998, 2017.

[37] J. P. Zuo, X. Wei, J. Wang, D. J. Liu, and F. Cui, "Investigation of failure mechanism and model for rocks in deep roadway under stress gradient effect," *Journal of China University of Mining and Technology*, vol. 47, no. 3, pp. 478–485, 2018.

[38] G. Li, F. Ma, G. Liu, H. Zhao, and J. Guo, "A strain-softening constitutive model of heterogeneous rock mass considering statistical damage and its application in numerical modeling of deep roadways," *Sustainability*, vol. 11, no. 8, 2019.

[39] Q. Li, J. Li, J. Zhang et al., "Numerical simulation analysis of new steel sets used for roadway support in coal mines," *Metals*, vol. 9, no. 5, 2019.

[40] S. Huang and S. Zheng, "Stressing state analysis of CFST arch supports in deep roadway based on NSF method," *Applied Sciences*, vol. 9, no. 20, 2019.

[41] Z. Xu, *Elasticity*, China Higher Education Press, Peking, China, 4th edition, 2006.

[42] C. Hou and P. Gou, "Mechanism study on strength enhancement for the rocks surrounding roadway supported by bolt," *Chinese Journal of Rock Mechanics and Engineering*, vol. 19, no. 3, pp. 342–345, 2000.

[43] W. Yu, B. Pan, F. Zhang, S. Yao, and F. Liu, "Deformation characteristics and determination of optimum supporting time of alteration rock mass in deep mine," *KSCE Journal of Civil Engineering*, vol. 23, no. 11, pp. 4921–4932, 2019.